AD-753 042

MEGAGAUSS PHYSICS

Heimo G. Latal

Foreign Technology Division
Wright-Patterson Air Force Base, Ohio

27 October 1972

DISTRIBUTED BY:

NTIS

National Technical Information Service
U. S. DEPARTMENT OF COMMERCE
5285 Port Royal Road, Springfield Va. 22151

AD753042

FTD-HT-23-1388-72

FOREIGN TECHNOLOGY DIVISION

MEGAGAUSS PHYSICS

by

Heimo G. Latal

D D C
RECEIVED
DEC 27 1972
D

Approved for public release;
distribution unlimited.

Reproduced by
NATIONAL TECHNICAL
INFORMATION SERVICE
U S Department of Commerce
Springfield VA 22151

UNCLASSIFIED
Security Classification

DOCUMENT CONTROL DATA - R & D

(Security classification of title, body of abstract and indexing annotation must be entered when the overall report is classified)

1. ORIGINATING ACTIVITY (Corporate author) Foreign Technology Division Air Force Systems Command U. S. Air Force	2a. REPORT SECURITY CLASSIFICATION UNCLASSIFIED 2b. GROUP

3. REPORT TITLE

MEGAGAUSS PHYSICS

4. DESCRIPTIVE NOTES (Type of report and inclusive dates)
Translation

5. AUTHOR(S) (First name, middle initial, last name)

Latal, H.G.

6. REPORT DATE 15 February 1971	7a. TOTAL NO. OF PAGES ~~26~~ 31	7b. NO. OF REFS 34
8a. CONTRACT OR GRANT NO. b. PROJECT NO. AP5H c. d.	9a. ORIGINATOR'S REPORT NUMBER(S) FTD-HT-23-1388-72 9b. OTHER REPORT NO(S) (Any other numbers that may be assigned this report)	

10. DISTRIBUTION STATEMENT

Approved for public release; distribution unlimited.

11. SUPPLEMENTARY NOTES Details of illustrations in this document may be better studied on microfiche.	12. SPONSORING MILITARY ACTIVITY Foreign Technology Division Wright-Patterson AFB, Ohio

13. ABSTRACT

Basically, this branch of physical research, which is concerned with the physics of megagauss fields, is considered as a rather technical development program. To a certain degree, however, interesting physical knowledge has been gained as a by-product of the generation method for these fields, which are primarily based on the behavior of metals under extreme conditions. In order to make reliable measurements possible, the technique of production of megagauss fields must first be brought to a level at which reproducible experiments are guaranteed.

I

DD FORM 1 NOV 65 1473

UNCLASSIFIED
Security Classification

14. KEY WORDS	LINK A		LINK B		LINK C	
	ROLE	WT	ROLE	WT	ROLE	WT
Metal Stress Magnetic Field Magnetic Pressure						

II

EDITED TRANSLATION

FTD-HT-23-1388-72

MEGAGAUSS PHYSICS

By: Heimo G. Latal

English pages: 26

Source: Acta Physica Austriaca, No. 34, 1971, pp. 65-82.

Requester: FTD/PDTN

Translated by: TSgt Fred A. Poole, Jr.

Approved for public release; distribution unlimited.

THIS TRANSLATION IS A RENDITION OF THE ORIGINAL FOREIGN TEXT WITHOUT ANY ANALYTICAL OR EDITORIAL COMMENT. STATEMENTS OR THEORIES ADVOCATED OR IMPLIED ARE THOSE OF THE SOURCE AND DO NOT NECESSARILY REFLECT THE POSITION OR OPINION OF THE FOREIGN TECHNOLOGY DIVISION.

PREPARED BY:

TRANSLATION DIVISION
FOREIGN TECHNOLOGY DIVISION
WP-AFB, OHIO.

Acta Physica Austriaca 34, 65-82 (1971)
Copyright by Springer-Verlag 1971

MEGAGAUSS PHYSICS

by

Heimo G. Latal

Institute for Theoretic Physics
University of Graz

with 5 figures

(Submitted on 15 February 1971)

FTD-HT-23-1388-72

IV

1. Introduction

Artificially produced magnetic fields of several million (MG) strength have become a reality in the past few years. This advance is mainly attributable to the fact that such fields were considered as one of the prerequisites for controlled fusion. For this reason, the corresponding research was secret in the beginning and only in the last ten years has this type of report appeared in freely accessable literature. Basically, this branch of physical research, which is concerned with the physics of megagauss fields, is considered as a rather technical development program. To a certain degree, however, interesting physical knowledge has been gained as a by-product of the generation methods for these fields, which are primarily based on the behavior of metals under extreme conditions. Other physical effects have also already been investigated (see Chapter 3). A great obstacle, from an experimental viewpoint, is given in part by the short duration of the fields (in the magnitude of μs), especially, however, by the more or less complete destruction of the experimental structure. In order to make reliable measurements possible, the technique of production of megagauss fields must first be brought to a level at which reproducible experiments are guaranteed.

The next Chapter concerns itself with these questions on the production of magnetic fields: first, the various methods and

their limits are discussed shortly and then extensively, the implosion methods ("flow compression") developed for achieving megagauss fields. In addition to the technique of flow compression, which uses explosives as a propellant, an interesting variation will also be discussed, that of electromagnetic compression. In the third chapter, physical measurements in megagauss fields, such as Zeeman and Faraday effects, and results for material parameters (for example, conductivity) under the extreme conditions prevailing in megagauss fields, are collected. The last chapter has as its content a special possibility of application of the megagauss fields for the investigation of highly energetic quantum electrodynamic effects.

2. Production of Megagauss Fields

The problems of production of ultra-high magnetic fields are of a multiple nature. Conventional direct current electromagnets with an iron core are significant only to field strengths of a maximal 30 kG, since then the iron is already completely magnetized. To achieve higher fields, iron cores can thus be foregone, whereupon, however, current consumption increases correspondingly. Thus, to obtain a 200 kG field, a few megawatts of power is necessary. In addition, an effective cooling system must be used as a result of the Joule heat which appears. Technical development in this respect culminated in the so-called "Bitter-Solenoid" [1]. Aside from the question of cost, these methods also have a set limit in fact that a magnetic field exerts a pressure on the current carrying conductor:

$$P(\text{kbar}) = 40\,B^2(\text{MG})$$

At 250 kG, the magnetic pressure reaches the flow limit of the metals and the coil can no longer purely mechanically resist these forces.

Superconductive magnets also, which are more favorable considering current consumption, but which require even more costly cooling systems, presently have their limits at approximately 150 kG, since this is the magnitude of the critical field strength which destroys the supraconduction.

Since the dynamic capacitance of metals is known to permit greater tolerances for pressure and heat, far higher fields can be momentarily produced through a pulsed operation. Thus, P. Kapitza, in 1925, succeeded in achieving field strengths of 320 kG for a few milliseconds, in that he short-circuited an alternating current generator for a half period with a small coil [2]. It then took 30 years until a new record was achieved with 750 kG [3]. The limits of the field strengths achievable through condenser discharges lie at approximately 2.5 MG, and in the meantime, fields of this strength have already been used in experiments (see Chapter 4).

Since the energy density of a megagauss field is comparable with the energy density of TNT, the thought was obvious, to produce magnetic fields in coils which are held together by explosives. The first theoretical suggestion in this direction originated from Terletzkii [4], which stated how one can amplify a beginning magnetic field through compression of a hollow conductor. These methods, which received the name "magnetic flow compression," were then further developed in secret in the USA as well as in the USSR, until the year 1960 when the first free accessible report appeared about it [5]. Meanwhile, successful flaw compressions were obtained in other laboratories as well [6]; in the following, we will especially go into the research program at the Illinois Institute of Technology in Chicago [7, 8, 9, 10, 11].

After these general observations, we will now concern ourselves in detail with magnetic flow compression. The principle of flow compression can be clearly illustrated with an example of

the supraconducting flow pump. We observe a long, hollow, cylindrical supraconductor, which encloses an axial magnetic field B, as is shown in Fig. 1. The currents, which the field contains, apparently flow in a layer thickness of the magnitude of the London depth of penetration λ_L [12]. We now use the Faraday induction law (μs units)

$$\oint \mathbf{E} \cdot d\mathbf{s} = -\frac{d}{dt} \int \mathbf{B} \cdot d\mathbf{A}. \tag{2.1}$$

on a cylinder up to a layer thickness δ, which should be about as large as λ_L. Then E ≈ 0 and the field behaves during profile changes as:

$$B_f = B_i \frac{A_i}{A_f}. \tag{2.2}$$

Thereby, we have neglected the axial variations (infinite solenoid) and assumed uniform field distribution over the profile A. This equation represents the fundamental formula for flow compression or expansion mechanisms. In principle, there apparently exists a symmetry between these two types of field changes, however, the flow expansion is much more effective and reduction factors in the magnitude of 10^5 have already been achieved [13], [14]. The difficulty of the reversion lies therein that the depth of penetration increases with the field and thus the effective surface relationship of a compression finally goes toward one.

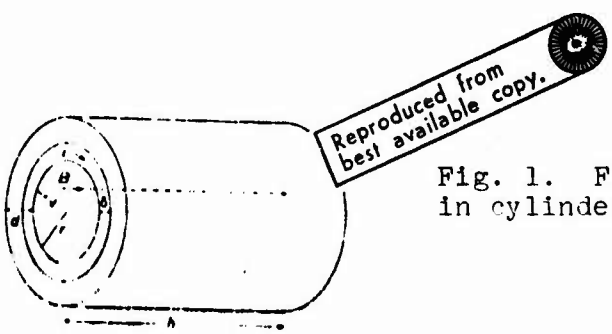

Reproduced from best available copy.

Fig. 1. Flow compression in cylinder geometry.

The transition from the supra-conducting to the normal flow compression is simple in concept. The difference exists therein that in the induction law (2.1), the left side does not disappear, but rather, in the Ohm and Ampere Law, is dependent on the field. In the first approximation, the left side is equal to $(2\pi r B_z \mu_0 \delta)$, whereby ρ is the specific resistance of the cylinder. In the event that the decrease of the profile takes place with constant speed v_0, we have

$$B_f = B_i \left(\frac{A_i}{A_f}\right)^{1-\beta}. \tag{2.3}$$

with

$$\beta = \frac{\rho}{\mu_0 \delta v_0}. \tag{2.4}$$

From equation (2.3) it is clear that an amplification of the field during profile decreasing can only be achieved if β is smaller than one; representative value for the resistance (a few $\mu\Omega$-cm) and the depth of penetration ($\sim$1 mm) lead therefrom to a lower limit for the speed v_0 in the magnitude of 0.1 km/s (= 0.1 mm/μs). This high speed of compression points in the direction of metallic cylinders deformed by explosives.

The main problem in the formulation of a satisfactory theory of flow compression lies therein that the dynamics of the cylinder is bound to the variation of the magnetic field through a non-linear system of differential equations with free edge conditions [see equation (2.5a, 2.5b)]. Thereby, the problem still depends additionally on the factor of the various solid body characteristics of the cylinder materials. Their behavior in megagauss fields is however, unknown and a complete theory must supply this as a part of the result. There are then, two practical possibilities of treating the problem. One consists thereof, that the necessary

information on cylinder characteristics in equations of condition and other physical relationships are combined and carefully extrapolated into the megagauss area. An electronic computer installation then simulates the compression, whereby the parameter set is varied so long until acceptable agreement with the experiment is achieved. A few examples of this method are described in [6].

The other way considers the variation of the cylinder parameters as the materially unknown of the problem. The increase of the field, and eventually the implosion dynamics also, are considered as input data and by data conversion, a set of parameters determined. From these phenomenologic theories, most of the results up to now have been obtained on the variation of the specific resistance of the cylinder (see Chapter 3).

Such a phenomenologic model was developed in [10]; it is based on the Faraday Induction Law (equation 2.1), whereby, very general assumptions on the current distribution were made and the energy flow balance between kinetic energy of the cylinder and produced electromagnetic energy. Thereby, the thickening of the cylinder wall was also considered, which resulted following the mass conservation of a cylinder assumed to be incompressible. Further, the fact is taken into account that only a fraction of the kinetic energy can be converted into electromagnetic energy, through the insertion of a phenomenologic efficiency ε. With the symbols from Fig. 1, we then obtain the two basic equations:

$$\frac{1}{B}\frac{dB}{dt} + \frac{2}{r}\frac{dr}{dt} + \frac{2\rho}{\mu_0 r^2 \ln(1 + \delta/r)} = 0, \qquad (2.5a)$$

$$r\frac{d^2r}{dt^2}\ln\left(1 + \frac{d_0(2r_0 + d_0)}{r^2}\right) + \left(\frac{dr}{dt}\right)^2\left[\ln\left(1 + \frac{d_0(2r_0 + d_0)}{r^2}\right) - \frac{r^2 d_0(2r_0 + d_0)}{r^2 + d_0(2r_0 + d_0)}\right] = \frac{\pi h d_0(2r_0 + d_0)}{\varepsilon\mu_0 m}B^2. \qquad (2.5b)$$

Her , ρ is the effective specific resistance of the cylinder material, m the total mass of the cylinder, d_0 and r_0 are the beginning values for the material thickness of the wall and for the inner radius of the cylinder. The three phenomenologic parameters of this model are primarily the specific resistance ρ, the depth of penetration of the current δ, and the effectiveness ε. For a comparison of various compressions, it is advantageous to make the equations independent of the beginning values by introducing dimensionless quantities. This occurs through the characteristic units of measure for length r_0 (beginning radius), time r_0/v_0 [$v_0 = -(dr/dt)_0$ is the beginning speed], and field B_0 (beginning field). Thereby, it is also appropriate, instead of the original set of parameters ρ, δ, ε, to introduce the quantities β, ν and η, which appear in the dimensionless equation in a natural manner:

$$\beta = \frac{\rho}{\mu_0 \delta v_0}, \tag{2.4}$$

$$\nu = \frac{\beta r_0}{\pi \delta}, \tag{2.6}$$

$$\eta = \frac{d}{\varepsilon}. \tag{2.7}$$

With a, we designate the relationship of original magnetic to kinetic energy:

$$a = \left(\frac{B_0^2 r_0^2 \pi h}{2\mu_0}\right) \Big/ \left(\tfrac{1}{2} m v_0^2\right). \tag{2.8}$$

Analytic solutions of the equation system (2.5a, 2.5b) are found for three special cases: for disregarding the concentration ($d << r$) for the flow compression in the approximation $\delta << r$ [10]; for the ideal ($\rho = 0$) compression [15]; and for the case of constant speed [10].

In the ideal compression (with d << r), the equation system (2.5a, 2.5b) is reduced to:

$$\frac{B}{B_0} = \left(\frac{r_0}{r}\right)^2. \tag{2.9a}$$

$$\frac{d^2r}{dt^2} = \eta v_0^2 \frac{r_0^2}{r^3}; \tag{2.9b}$$

which has the solution

$$r = r_0\left[1 - 2\frac{v_0}{r_0}t + (1+\eta)\left(\frac{v_0}{r_0}t\right)^2\right]^{1/2}. \tag{2.10a}$$

$$B = B_0\left[1 - 2\frac{v_0}{r_0}t + (1+\eta)\left(\frac{v_0}{r_0}t\right)^2\right]^{-1}. \tag{2.10b}$$

It follows therefrom, that a maximal field

$$B_m = B_0\frac{1+\eta}{\eta}. \tag{2.11a}$$

with a radius of

$$r_m = r_0\sqrt{\eta/(1+\eta)}. \tag{2.11b}$$

at time

$$t_m = \frac{r_0}{v_0}(1+\eta)^{-1}, \tag{2.11c}$$

is achieved.

If the finite conductivity of the cylinder is considered, in contrast, thus the situation complicates itself by leaps and bounds, even under the simplifying assumption that the depth of penetration of the current is very small as opposed to the radius of the cylinder ($\delta << r$). Instead of the simple relationship (2.9a) between field and radius, we now obtain

$$\frac{B}{B_0} = \left(\frac{r_0}{r}\right)^2 \exp\left\{-2\beta v_0 \int_0^t \frac{dt'}{r(t')}\right\}. \tag{2.12a}$$

while the dynamics is determined by the differential equation:

$$r\frac{d^2r}{dt^2} + \frac{d^2r}{dt^2}\left|3\frac{dr}{dt} + 4\beta v_0\right| = 0. \tag{2.12b}$$

The integration of (2.12b) leads to a differential equation of the Abel type, which solution, however, joins r and t only in am implicit form. If we introduce the speed $v = -(dr/dt)$ as a new independent variable, thus we obtain as a solution for (2.12b)

$$r = r_0\left|\frac{\eta v_0^2}{(1+\eta-4\beta)v_0^2 + 4\beta v_0 v - v^2}\right|^{1/2} \times \left|\frac{v - v_e}{v - \tilde{v}_e}\frac{v_0 - \tilde{v}_e}{v_0 - v_e}\right|^{\cdots(1\ 2\beta v_0)^{1/2}}, \tag{2.13}$$

Reproduced from best available copy.

with the abbreviation

$$\begin{matrix}\tilde{v}_e \\ v_e\end{matrix}\Big| = v_0\{2\beta \pm [(1-2\beta)^2 + \eta]^{1/2}\}.$$

The solution (2.13) is valid for the area $0 \leq v_e \leq v \leq v_0$. For the numerical computation, it is advantageous to consider the speed v as an independent variable, to compute the radius from (2.13), and finally to obtain the appropriate time from:

$$t = \frac{r_0 v_0 - rv - 4\beta v_0(r_0 - r)}{(1+\eta-4\beta)v_0^2}. \tag{2.14}$$

The field can then be computed as a function of time by means of the relationship:

$$\frac{B}{B_0} = \frac{r_0}{r}\left[\frac{(1+\eta-4\beta v_0^2+4\beta v_0 - v^2)}{\eta v_0^2}\right]^{1/2} \tag{2.15}$$

Reproduced from best available copy.

Thereby, it is interesting to discover that in general, great variations in r are connected with only small changes in v over a great part of the compression time. Toward the end of the compression, however, the opposite is the case: while v goes practically from v_0 toward null, r remains almost constant. It is clear that such a relationship can be described only with difficulty by a simple analytical function, and therefore such a complicated form as (2.13) is necessary.

As a further illustration, the case of compression with constant speed is also discussed. The dynamics is thus given

$$r = r_0 - v_0 t, \tag{2.16a}$$

Equation (2.5b) is therefore cancelled, and we obtain

$$\frac{B}{B_0} = \left(\frac{r_0}{r}\right)^2 \exp\left\{-2\beta\left[li\left(1+\frac{\delta}{r}\right) - li\left(1+\frac{\delta}{r_0}\right)\right]\right\}. \tag{2.16b}$$

whereby the integral logarithm is used:

$$li(z) = \int_0^z \frac{dx}{\ln x}$$

If we again assume the depth of penetration δ is small as opposed to r, thus we can write (2.16b) approximately:

$$\frac{B}{B_0} \cong \left(\frac{r_0}{r}\right)^{2(1-\beta)}\left[1+0\left(\beta\frac{\delta}{r}\right)\right]. \tag{2.17}$$

This result shows that for the case of constant speed, even with finite conductivity, an exponential law such as (2.9a) again follows, only that the exponent is changed from 2 to $2(1 - \beta)$ (compare also (2.3)). It is also interesting to note that the enclosed flow in this case can easily be computed, it decreases as

$$\phi(r) = \phi(r_0)(r/r_0)^{2\beta}. \tag{2.18}$$

thereby, the name "flow compression" is found to be somewhat misleading, since the flow can, at most, remain constant.

As a further result of these computations, it is shown that it is appropriate to consider not only the chronological progress of the field B(t) and its time derivation dB/dt, but rather also various simple combinations of the two functions. Thus, for example, a series development according to exponents of time is not logical for B or for dB/dt, since these converge extremely poorly. In contrast, the linear approximation

$$B_0/B \cong 1 - (1 - \beta)\frac{v_0}{r_0}t + O\left(\beta\frac{v_0^2}{r_0^2}t^2\right) \tag{2.19}$$

shows extraordinary good agreement with the experimental data for approximately 50% of the total compression time. In an analog manner, one also finds in the combination B/(dB/dt) a linear decline over the greatest part of the flow compression, which is terminated with a sharply defined minimum. The combination $B^{-3/2}(dB/dt)$, which in the ideal case is proportional to speed,

$$B^{-3/2}(dB/dt)_{ideal} = \frac{2}{r_0 B_0^{1/2}}. \tag{2.20}$$

in general possesses a distinct maximum, which chronologically lies in front of the minimum of B/(dB/dt). And finally, one obtains also for $B^{-2}(dB/dt)$ a linear range in the beginning, for the case of ideal compression, this combination is even a strictly linear function of time,

$$\left[B^{-2}(dB/dt)\right]_{ideal} = \frac{2}{B_0 r_0}\left|1 - (1+\eta)\frac{v_0}{r_0}t\right|. \qquad (2.21)$$

From the characteristic behavior and the empirically found fact that for each of these combinations, a well-defined point of time exists at which the function is independent from β (within certain limits), the variation of the parameter set β, η, ν can be determined with relatively small cost [11]. The most important results of the analysis of typical flow compression experiments with assistance of this model are described in Chapter 3.

Naturally, of especial interest is the maximal achievaable field for a given set of parameters. Thereby, it is shown that for small η, the availability of a resistance ($\beta \neq 0$) even increases in the beginning the maximal compression relationship B_m/B_0, in contrast to the nondissipative case (2.11a), however, for further increasing β, the possible field enlargement decreases again, and for $\beta \to 1$, also goes toward one.

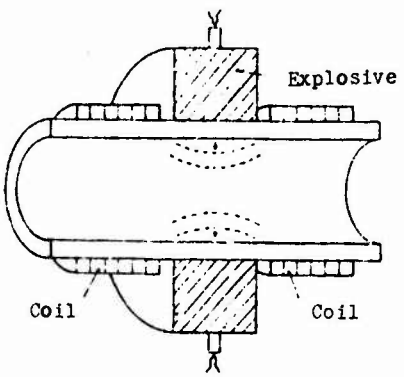

Fig. 2. Cylindrical implosion.

Two variations of implosion configurations with explosives were used in the experiments at the Illinois Institute of Technology. In Fig. 2, the construction of a cylindric compression is schematically shown. The beginning field is produced through a Helmholtz coil system, which, however, in the experiments carried out was not very effective and only permitted achieveing beginning fields of about 10 kG. The dimensions of the stainless steel cylinder were: inner diameter 10.2 cm, wall thickness 3.2 mm, length 23 cm. With approximately 3 kg explosive ("Composition B") an end field of somewhat over 1 MG was achieved.

The other variation is a conical compression, which is indicated in Fig. 3. Here, the beginning field was produced by a solenoid (about 60 kG) and then the cylinder of stainless steel was conically compressed by an explosion progressing from top to bottom. This configuration is especially little susceptable to interference and therefore permits reproducible results; thus, for example, in five of seven comparable compressions, fields between 3.2 MG and 3.6 MG were obtained from profiles with diameters of 4 to 5 mm. The time between beginning of the field increase and achievement of the maximal field also varies extremely little and lies at (21 ± 1) μs. With this arrangement, which was developed by F. Herlach, reproducible experiments would already be possible in principle. Thus, for example, the Faraday effect was measured up to 2 MG (see Chapter 3).

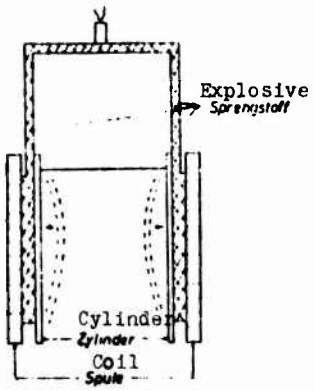

Fig. 3. Conical implosion.

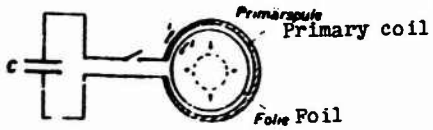

Fig. 4. Electromagnetic compression.

In general, however, the necessity of using explosives and the dangers connected thereto limit the possibilities of use of such explosive compressions. For this reason, the discovery by Cnare [16] that magnetic flow compression of a pure electromagnetic type is possible, meant an interesting new direction in this area. As presented in Fig. 4, the construction is relatively simple. The role of the cylinder is taken over by a thin aluminum foil and the explosive is replaced by a massive primary coil. When, now, the condenser battery discharges through the primary windings, so counter-directed, equal currents flow in the primary and secondary circuits, because of the narrow coupling. As is known, these are mutually repulsing, the foil is imploded because of the mechanical asymmetry of the system, whereby speeds in the range of 1 mm/μs and more are achievable. During the implosion, the magnetic field produced by the primary coil can diffuse inside and is then amplified in the same manner as with the explosive compression [17]. In the tests carried out up to now, the achieved field strengths lie at about 1 to 2 MG with profiles of about 3 mm diameter [18, 31]. With these methods of electromagnetic compression, which are far less dangerous, less destructive and additionally, costs less than its explosive analogs, a broader physical research with megagauss fields could be possible some day. One of the new possible uses is treated in Chapter 4.

3. Application of Megagauss Fields

As already mentioned earlier, up to now the possible uses of artifically produced fields in the megagauss range were very

limited, since only few institutes had the necessary prerequisites for this type of research and, in addition, the technique of production of these fields has only lately been brought to a state which permits reproducable experiments. For this reason, the most important results were obtained mainly in the area of material constants of metals in megagauss fields, while the isolated measurements of the Faraday and Zeeman effects formed a step in the direction of actual applications.

In the characteristics of metalic cylinders, which are used for production of the fields, the specific resistance and the effectiveness ε mainly play a decisive role. These quantities are determined from the analysis of seven comparable flow compression experiments with the assistance of the phenomenological model (equation 2.5a, 2.5b) [11]. In the "linear range," that is, where B/(dB/dt), etc., are linear functions of time, values around 100 $\mu\Omega$-cm were obtained for the specific resistance of the steel cylinder. This agreed with expectations, since in this area there is independent, still experimental data available. Interestingly, the specific resistance increases only by a factor of two, even in fields of more than 3 MG, that is, a value of approximately 200 $\mu\Omega$-cm results as the upper limit for the steel cylinder used. A satisfactory theoretical explanation of this low resistance has still not been found. The effectiveness ε could also be determined relatively well, it is essentially constant and lies at 30% to 50% for the investigated case. In order to be able to physically interpret this data won from the analysis of the experiments, additional theoretical assumptions, which pass beyond the framework of the simple phenomenological model (equation 2.5a, 2.5b), had to be made.

In contrast to the above mentioned results on the material parameters, the measurements of the Faraday and Zeeman effects represent the first experiments in megagauss fields, although

they were primarily thought of as supplemental diagnostics of the field progression. The Faraday effect, as is known, is the rotation of the polarization plane of a light beam in a homogeneous isotrope medium as a result of a magnetic field laid parallel to the light beam. The rotation angle 0 stands in relationship with the field B

$$\theta = VlB. \qquad (3.1)$$

whereby l is the length of the path in the medium (and magnetic field) and V is the so-called Verdet constant. From dispersion-theoretical considerations [19], the Verdet constants are dependent on the material parameters and the wavelength of the light used, it is, however, (for fields smaller than 100 MG) field-independent, in the materials investigated (glass, quartz). Detailed measurements of these linear Faraday effects were made up to field strength of 2 MG [20], the field progression obtained therefrom agrees with the measured values from the usual induction sensors within the experimental error limits.

In the same way, the measurement of the Zeeman effect [21] essentially serves for testing a further method of determining the magnetic field in an implosion. Exploding wires, which were adulterated with various salts, were used as a light source. As especially favorable were the sodium-D line (5839 Å) and the line of indium at 4102 Å, in which doublet splitting parallel to the field was observed. Thereby, in one case, splitting resulted in 120 Å (sodium) and 79 Å (indium), which corresponds to a magnetic field of 3.7 MG; in another compression which achieved 5.1 MG, the maximal splitting of the sodium line amounted to 164 Å. Here, also, the best agreement was shown between these field measurements and those from induction tests.

From this discussion, it is clear to see that the area of the use of megagauss fields in physics is only in the beginning

stage and the possibilities have not all been determined, by far. Views of further megagauss experiments in solid body physics are presented in [22] and [23]; a special possibility of use in high energy physics is the content of the following chapter.

4. Quantum Electrodynamics in High Magnetic Fields

A complete theory of the reciprocal effect of electrons with the electromagnetic field must contain, in the classical framework as well as in the quantum-mechanical, treatment of the effects of the radiation damping. Usually, these are only small corrections, except in the cases in which extremely great accelerations occur. Such movement changes can only be caused by strong fields, whereby, in this connection, strong means that the field strengths with the natural quantum-mechanical field strengths

$$\left.\begin{matrix} E_{cr} \\ H_{cr} \end{matrix}\right| = \frac{m^2c^3}{eh} = \left.\begin{matrix} 1{,}32 \times 10^{16}\ \mathrm{V/cm} \\ 4{,}41 \times 10^{13}\ \mathrm{G} \end{matrix}\right| \qquad (4.1)$$

are comparable. In theoretical respects, the problem of the strong radiation damping effects is not very satisfactory; the classical theory has to contend with pre-accelerations, exponentiai increasing and unstable solutions [24], while in the simple quantum-mechanical models investigated up to now, among other things, antimated "ghost behavior" and acausalties occur [25]. A logical way out of these difficulties would be suitable unambiguous experiments, which execution up to now has failed because of the size of the field strengths necessary (equation 4.1). Althcugh electrical fields of the magnitude of (equation 4.1) occur, for example in the Lamb-displacement in heavy elements or in vacuum polarization effects in μ-mesic atoms, these experiments, because of their multipartical and nuclear physical nature,

are bound to difficult-to-estimate uncertainties. Only with the successful production of artificial magnetic fields in the megagauss range, coupled with electron energies in the magnitude of many GeV, can now the first steps be made in the experimental clarification of the problem [26]. That high energies are also of importance in this connection can be noted in that an electron with the energy E in a stationary magnetic field H sees an effective field $(E/mc^2)H$. For H = 10 MG and E = 20 GeV, this field is only more than two magnitudes smaller than H_{cr} in equation (4.1).

The simplest electromagnetic conversion process in an outer magnetic field is the magnetic radiative stopping (synchrotron radiation). This process was investigated in detail in the framework of the classical as well as in the quantummechanical theory [27, 28, 29, 30], to be sure, without consideration of the radiation damping. When extremely relativistic electrons of the energy E transit a path Δ vertical to a magnetic field H, thus the total radiated radiative stopping energy is

$$I(H, E, \Delta) = \frac{2}{3}\alpha \frac{mc^2}{\lambda_c}\left(\frac{E}{mc^2}\frac{H}{H_{cr}}\right)^2 \Delta. \qquad (4.2)$$

whereby α = 1/137 and λ_c = h/mc are the Compton wave length of the electron. In the same way, the total number of the photons radiated per electron can be computed as

$$N(H, E, \Delta) = \frac{5}{2\sqrt{3}}\alpha \frac{1}{\lambda_c}\frac{H}{H_{cr}}\Delta. \qquad (4.3)$$

which mean energy is given by

$$\langle h\omega \rangle = \frac{4}{5\sqrt{3}} E\left(\frac{E}{mc^2}\frac{H}{H_{cr}}\right). \qquad (4.4)$$

Numerical values for these quantities will be discussed later in the closing of the description of a series of experiments at the Stanford Linear Accelerator Center. Thereby, for the first time megagauss fields were used as targets of the high energetic electron beam and the radiation under these conditions was measured [31].

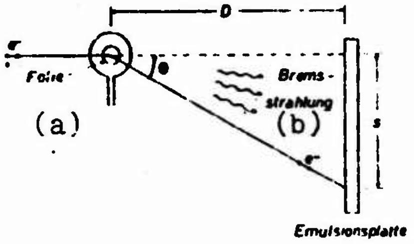

(c)

Fig. 5. Radiative stopping experiment.
KEY: (a) Foil; (b) Radiative stopping; (c) Emulsion plate.

The schematic construction of such an experiment is shown in Fig. 5. A package of high energetic electrons is shot into the megagauss field which maximal value is synchronized chronologically exact with the electron beam. Thereby, deviations of 0.1 μs at most can be tolerated. In relation to spacial synchronization also, high demands are placed: the electron beam has a thickness from 0.5 to 1 mm (vertical to direction of movement) and is supposed to strike the center of the magnetic field with a deviation of less than 0.5 mm, which extends over a range of 3 to 4 mm. During the deflection in the magnetic field, the electrons emit radiative stopping quantum, which are mainly beamed in the forward direction (the main part of the emission, as is known, lies within a sphere with an aperature angle $mc^2/E \simeq 10^{-5}$ rad). The photons are distributed essentially only over the deflection angle of the electrons

$$\theta_0 \quad \frac{A\,H\,mc^2}{\lambda_c H_0\, E} \qquad (4.5)$$

in one direction, while in the other direction, practically only the width of the electron beam at the location of the magnetic field is pictured on the emulsion plate. As a result of the small spatial spread and the sharp energy spectrum of the electron beam, a small split occurs in the magnetic field, so that the deflected beam overlaps the radiative stopping spectrum by only a fraction on the emulsion plate.

From June to November 1970, 15 successful tests were carried out, of which seven are counted as actual experiments, the remaining eight were test arrangements. The electron beam contained 0.5 to 5 × 10^6 electrons per pulse with an energy of 19 GeV. In five of the seven experiments, the magnetic fields were produced by discharge of a 60 kJ condenser battery in small coils, the fields achieved thereby were 1.2 to 1.7 MG from diameters of 3 to 4 mm. Two of the experiments were electromagnetic compressions, which delivered 1.6 to 2.0 MG from 3.5 mm. From equation (4.5), one can see that for these conditions, the deflection angle θ_0 of the electrons lies at 10^{-2} rad; to be able tc register a good measureable deflection, the emulsion plates were positioned approximately 15 m (=D in Fig. 5) from the megagauss target.

According to equation (4.2), a total energy in the magnitude of 100 MeV was emitted in these experiments, thus, 0.5% of the electron energy. Since N from equation (4.3) is approximately 5, thus 10^6 to 10^7 radiative stopping photons with a mean energy of 18 MeV (see equation (4.4)) is expected. A comparison with the newest measurements to date of the synchrotron emission in Frascati [32] and Hamburg [33], in which photons of a maximal 0.2 keV and 0.3 MeV were reached, shows that the here mentioned experiments with megagauss fields expand this range by several magnitudes. This fact, together with the introduction of megagauss fields as targets in high energy physics, was the main motivation for carrying out these tests, which results are now being evaluated.

In addition, the possibility was principally not excluded, thereby to be able to observe the radiation emission effect. The governing parameter for the magnitude of this correction is the relationship of emission reaction force and Lorentz force: extensively independent of the model, it results in

$$\delta \approx \frac{2}{3}\left(\frac{E}{mc^2}\right)^2\left(\frac{H}{H_{cr}}\right) \qquad (4.6)$$

and strong radiation damping indicates $\delta \gtrsim 1$. A second correction which changes the classic results, arises through the increasing influence from quantum effects, that is, when the energy of the radiated photons is comparable with the electron energy. From equation (4.4) we see that this leads to the requirement

$$\chi \approx \frac{E}{mc^2}\frac{H}{H_{cr}} \ll 1. \qquad (4.7)$$

An interesting characteristic of the magnetic radiative stopping exists in that it is possible, through suitable selection of electron energy and magnetic field strength, to achieve strong emission damping effects *without* quantum corrections. According to equation (4.7), the latter are small, when

$$\chi \ll 1, \qquad (4.8a)$$

while strong emission damping, according to equation (4.6) means

$$\delta \gtrsim 1. \qquad (4.8b)$$

Both requirements could be fullfilled simultaneously, if the electron energy is so large that

$$\frac{E}{mc^2} \gg \frac{1}{\alpha} = 137, \qquad (4.8c)$$

thus, it lies in the magnitude of several GeV.

For the special case of the above described experiment (E = 20 GeV, H = 2 MG), equation (4.8c) is certainly satisfied, the parameter for quantum effects and emission damping are $y \simeq 2 \times 10^{-3}$ and $\delta \simeq 0.4$. For this reason, the problem can be treated in the framework of the classic theory of the emission damping. In the Lorentz-covariant form, the movement equation of an electron in an electromagnetic field, considering the radiation reaction, reads

$$\dot{u}_\mu = \frac{e}{mc} F_{\mu\nu} u^\nu + \tau_0 \left| \ddot{u}_\mu - \frac{1}{c^2} u_\mu (\dot{u}^\nu \dot{u}_\nu) \right| \cdot \qquad (4.9)$$

Reproduced from best available copy.

Thereby u_μ is the four-velocity of the electron, $F_{\mu\nu}$ is the electromagnetic field tensor, $\dot{u}_\mu = du_\mu/d\tau$ is the derivation of the four-velocity according to the proper time $d\tau$, and $\tau_0 = 2e^2/3mc^3$ is the characteristic radiation reaction parameter. The first term on the right side of equation (4.9) is the usual Lorentz force, while the two remaining expressions describe the force which arises through the reaction of the radiated electromagnetic field on the electron. An extensive discussion of the derivation of this equation and its validity can be found in [24].

A method of approximately solving this problem, and thereby still consider the strong radiation reaction effect, was developed by Shen [34]. The term $(\dot{u}^\nu \dot{u}_\nu)$ in equation (4.9), which makes this equation non-linear, is obviously a Lorentz scalar and thus has the same value in every Lorentz system, even in the momentary rest system of the electron. Under the prerequisites of equation (4.8) and with the assumption that the magnetic field H is vertical to the direction of incidence of the electron,

this term can be approximately computed, whereby only the lowest arrangements in (mc^2/E) and y are carried, however δ can also be greater than one. After a transformation in the observer system, one obtains in this approximation for the two velocity components vertical to the magnetic field

$$v_1 \approx v_0 \exp\left[-h(t)\right] \cos f(t), \tag{4.10a}$$

$$v_2 \approx v_0 \exp\left[-h(t)\right] \sin f(t). \tag{4.10b}$$

Thereby, v_0 is the beginning velocity and

$$h(t) \cong \frac{8}{3}\alpha\left(\frac{mc^2}{E}\right)\left(\frac{H}{H_{cr}}\right)^2 \frac{ct}{\lambda_c}. \tag{4.11a}$$

$$f(t) \cong \left[1 + \frac{\alpha}{3}\left(\frac{E}{mc^2}\right)\left(\frac{H}{H_{cr}}\right)^2 \frac{ct}{\lambda_c}\right]\left(\frac{mc^2}{E}\right)\left(\frac{H}{H_{cr}}\right)\frac{ct}{\lambda_c}. \tag{4.11b}$$

From these results, the deflection angle of the electrons can now be computed:

$$\theta \approx \theta_0 + \theta_1 \approx \arctan f(t_0), \tag{4.12}$$

whereby θ_0 is the angle of equation (4.5) without radiation reaction and $t_0 = \Delta/v_0 \cong \Delta/c$ is the transition time through the magnetic field. For the values of the above described radiative stopping experiment, $f(t_0) << 1$ and we obtain therefore, for the additional deflection

$$\theta_1 \sim \frac{\alpha}{3}\left(\frac{H}{H_{cr}}\right)^3\left(\frac{\Delta}{\lambda_c}\right)^2. \tag{4.13}$$

With E = 20 GeV, H = 2 MG and Δ = 5 mm, the procentual change of the deflection angle amounts to about 0.25%, and this means

a displacement of the electron beam of about 0.4 mm at a total deflection of 22.2 cm on the emulsion plate located 15 m away (= s in Fig. 5). Since, however, as a result of the spatial distribution of the electrons in the beam, this produces a spot of several cm diameter on the plate, the correction (equation 4.13) is not measurable. One of the possibilities to possibly make this effect visible, would be the measurement of the deflection of sharply focussed nanosecond pulses, which are composed of a mixture of electrons of the energy E and heavy relativistic particles (for example, μ-mesons) of the energy E'. Since according to equation (4.13), θ_1 does not depend on particle energy, but is reversely proportional to the fourth power of the mass, the heavy particles could be drawn in for the calibration of the primary deflection, against which, then, the additional deflection of the electrons would be measurable as a result of the radiation reaction.

In contrast to the influence of the radiation reaction on the electron deflection, the computation of the effects on the radiative stopping spectrum affords a materially greater display. For the case that several cycles are observed, the appropriate results are given in [34], for the mentioned radiative stopping experiments, the electrons remain only a thousandth part of a full cycle in the magnetic field, which brings additional difficulties. Computations in this direction are presently being made.

In closing this discussion, it can be said that megagauss fields as targets have successfully been introduced in high energy physics, and thereby the range existing for the measurement of the classic synchrotron radiation, could be expanded a number of magnitudes. Thereby, the first step has been made in the direction of an experimental verification of the radiation

reaction effect, although measurable deviations will first be observable in even higher energies and fields, but perhaps also through refined measuring methods in the presently accessable range.

At this point I would like to express my sincere thanks to my honored teacher, Professor Dr. Paul Urban, for his generous support and continuous advancement. I thank Professor Dr. Thomas Erber for his most friendly hosting during my stay at the Illinois Institute of Technology, Chicago. I am indebted to him and Professor Dr. Fritz Herlach for many stimulating discussions. Parts of this work were supported by the U. S. Army Research Office (Durham) and the National Science Foundation.

BIBLIOGRAPHY

1. F. Butler, Rev. Sci. Instr. 10, 373 (1939).
2. P. Kapitza, Proc. Soc. A 115, 658 (1927).
3. S. S. Foner and H. H. Kolm, Rev. Sci. Instr. 27, 547 (1956).
4. Ia. P. Terletzkii, Sov. Phys. JETP 32, 301 (1957).
5. C. M. Fowler, W. B. Garn and R. S. Caird, J. Appl. Phys. 31, 588 (1960).
6. Siehe: Proceedings of the Conference on Megagauss Magnetic Field Generation by Explosives and Related Experiments, Frascati (Italy) 1965 (H. Knoepfel and F. Herlach, eds.). Euratom report EUR 2750 e.
7. T. Erber, G. K. Forsioros, H. G. Latal, J. A. Mazzu and J. E. Kennedy, Les Champs Magnetiques Intenses, p. 335. Paris: CNRS. 1967.
8. H. G. Latal, F. Herlach und T. Erber, Bull. Am. Phys. Soc. 15, 72 (1970).
9. J. E. Kennedy und F. Herlach, Bull. Am. Phys. Soc. 15, 98 (1970).
10. T. Erber und H. G. Latal, Reports on Progress in Physics 33 (im Druck).
11. T. Erber und H. G. Latal (in Vorbereitung).
12. H. B. G. Casimir und J. Ubbink, Philips Techn. Rev. 28, 300 (1967).
13. R. E. Brown und W. M. Hubbard, Rev. Sci. Instr. 36, 1378 (1965).
14. R. E. Brown, Rev. Sci. Instr. 39, 517 (1968).
15. T. Erber, H. G. Latal und P. Urban, Sitzungsber. d. Österr. Akad. Wiss. 178, 25 (1969).
16. E. C. Evans, J. Appl. Phys. 37, 3812 (1966).
17. H. G. Latal, Ann. Phys. (N.Y.) 42, 352 (1967).
18. D. Kachelen, F. Herlach und T. Erber, Rev. Sci. Instr. 41, 1 (1970).
19. A. Sommerfeld, Vorlesungen über Theoretische Physik, Band IV (Optik), 2. Aufl., S. 89. Leipzig: Akademische Verlagsgesellschaft. 1959.
20. F. Herlach, H. Knoepfel, R. Lecercq und J. L. Van Montfoort, S. 473 in 6.
21. W. B. Garn, R. S. Caird, D. B. Thomson und C. M. Fowler, Rev. Sci. Instr. 37, 762 (1966).

Reproduced from best available copy.

22. J. L. Olsen, S. 483 in „G".
23. F. Herlach, Helvetica Physica Acta 41, 808 (1968).
24. T. Erber, Fortschr. d. Physik 9, 343 (1961).
25. S. Coleman and R. E. Norton, Phys. Rev. 125, 1122 (1962).
26. T. Erber, Zeitschr. f. Angew. Phys. 21, 388 (1968).
27. A. A. Sokolov und I. M. Ternov, Synchrotron Radiation. Berlin: Akademie-Verlag. 1968.
28. T. Erber, Rev. Mod. Phys. 38, 626 (1966).
29. N. P. Klepikov, Zh. Eksperim i Teor. Fiz. 26, 19 (1954).
30. J. J. Klein, Rev. Mod. Phys. 40, 523 (1968).
31. T. Erber und F. Herlach et al. (in Vorbereitung).
32. G. Missoni und A. Ruggiero, Rend. Acad. Lincei 38, 677 (1965).
33. G. Bathow, E. Freytag und R. Haensel, J. Appl. Phys. 37, 3449 (1966).
34. C. S. Shen, Phys. Rev. Lett. 24, 410 (1970).

Printed in Austria

Reproduced from best available copy.